Mild hydrogenation of quinoline
2. A novel Rh-containing pillared layered clay catalyst

M. Campanati [a], M. Casagrande [b], I. Fagiolino [a], M. Lenarda [b], L. Storaro [b],
M. Battagliarin [c], A. Vaccari [a],*

[a] *Dipartimento di Chimica Industriale e dei Materiali, INSTM Udr di Bologna, Viale Risorgimento 4, 40136 Bologna, Italy*
[b] *Dipartimento di Chimica, Università Ca'Foscari di Venezia, INSTM UdR di Venezia, Via Torino 155/B, 30100 Mestre-Venezia, Italy*
[c] *Dipartimento di Chimica Fisica, Università Ca'Foscari di Venezia, INSTM UdR di Venezia, Via Torino 155/B, 30100 Mestre-Venezia, Italy*

Abstract

A novel highly dispersed Rh-containing catalyst (Rh, 2 wt.%) was prepared by ion-exchange of a Mg/Al/Ce pillared montmorillonite and characterized by chemical analysis, X-ray diffraction analysis and H_2 chemisorption. The Rh crystallites which formed were smaller than 2 nm. The catalytic behavior of this Rh-containing pillared layered clay (Rh–PLC) catalyst was investigated in the mild hydrogenation of quinoline ($T = 373$–473 K; $P_{H_2} = 2.0$ MPa) and compared with that of a commercial 5 wt.% Rh on alumina (Rh–Al_2O_3) catalyst. At 373 K, both catalysts gave only partial hydrogenation to 1,2,3,4-tetrahydroquinoline (py-THQ), although with a significantly lower conversion for Rh–PLC, attributable to its microporous structure and steric hindrance of quinoline. However, when the temperature was increased to 473 K, Rh–PLC, unlike the commercial catalyst, was able to fully hydrogenate quinoline to decahydroquinoline, underlining the key role played by the metal particle size. © 2002 Elsevier Science B.V. All rights reserved.

Keywords: Quinoline; Mild hydrogenation; Rh; Pillared layered clay; Metal dispersion

1. Introduction

The hydrogenation of quinoline and its derivatives is of high industrial relevance, with applications in the petrochemical, fine chemical and pharmaceutical industries [1–4]. Heterogeneous catalysts containing different metals (Pd, Ni, Rh, Pt, Cu, etc.) have been tested in the liquid phase for the complete hydrogenation of quinoline to decahydroquinoline (DHQ) which was found to occur with two different reaction steps [5]. The first one is the formation mainly of 1,2,3,4-tetrahydroquinoline (py-THQ), while the second is the complete hydrogenation of py-THQ to DHQ (Fig. 1). The reaction conditions required for the first step include reaction temperatures up to 373 K and hydrogen pressure from 0.1 to 7.0 MPa, using an alcohol as the solvent [6–8]. The conversion of py-THQ to DHQ requires longer reaction times and more drastic reaction conditions, typically a temperature in the range 448–533 K, hydrogen pressure between 11.0 and 21.0 MPa and the use of a strong Brönsted acid as the solvent [9,10]. The role of the reaction parameters in mild hydrogenation of quinoline has been investigated using different noble metals (Pd, Rh, Ru)-based commercial catalysts, evidencing in all cases only partial hydrogenation to py-THQ [11]. This catalyst

* Corresponding author. Tel.: +39-051-209-3683;
fax: +39-051-209-3680.
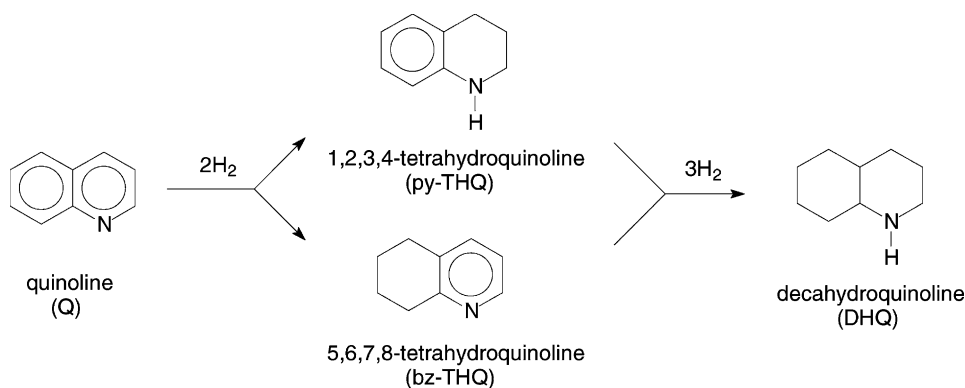*E-mail address:* vacange@ms.fci.unibo.it (A. Vaccari).

Fig. 1. Reaction pathway for quinoline hydrogenation.

deactivation during the first step hydrogenation to py-THQ may be attributed to the adsorption of reaction intermediate(s) on the active sites. Moreover, a possible way to remove this effect was the addition of a Lewis base to the reaction mixture, which favored complete hydrogenation by competitive adsorption on the catalyst surface.

Another possible way to smooth the catalyst deactivation may be the use of highly dispersed metal catalysts, analogous to that observed in the stereoselective hydrogenation of methyl pyruvate using a Pt–cinchonidine heterogeneous catalyst [12]. When the Pt crystallites were smaller than 4 nm, a decrease in enantioselectivity was observed and attributed to a decrease in the adsorption on the metal surface of the quinolinic ring of cinchonidine [13–15]. The aim of the research reported here was to shed light on the role of the metal particle size, by preparing a highly dispersed Rh-containing pillared layered clay (Rh–PLC) catalyst and checking its activity in the mild hydrogenation of quinoline. For comparison, a commercial Rh/Al$_2$O$_3$ catalyst was also investigated in the same conditions.

2. Experimental

Flego et al. [16] reported that a montmorillonite pillared with mixed Al/Ce/Mg polyoxocations gave rise to quite thermally resistant materials, therefore, the synthetic procedure described was applied in the preparation of the pillared clay support. To

500 ml of a solution containing AlCl$_3$ (0.125 mol), Ce(NO$_3$)$_3$·6H$_2$O (0.016 mol) and Mg(NO$_3$)$_2$·6H$_2$O (0.019 mol), a total of 320 ml of 1 M NaOH solution was slowly added under vigorous stirring. The resulting clear solution obtained was first aged for 3 h at 333 K and then 15.0 g of dry Ca-montmorillonite (Detercal P1-Laviosa) were slowly added under vigorous stirring. This mixture was mechanically stirred for 2 h at 333 K and for 48 h at room temperature, then it was centrifuged and washed with distilled water until free of Cl$^-$ ions (AgNO$_3$ test). The washed clay was dried at 373 K for 12 h, then ground and calcined in a muffle furnace under air flow at 823 K for 24 h to form the PLC.

A total of 2 g of PLC (mesh 60–120) were added to 170 ml of an aqueous solution containing 0.116 g of [Rh(NH$_3$)$_5$Cl]Cl$_2$. The mixture was stirred for 4 days at room temperature, then washed with distilled water until free of Cl$^-$ ions (AgNO$_3$ test). The rhodium loading, determined by atomic absorption spectroscopy was 2 wt.%. The Rh–PLC catalyst was dried at 373 K for 12 h, then ground and calcined in a glass reactor at 673 K for 12 h (air flow = 80 ml/min, heating rate = 1 K/min) followed by cooling under He flow, then reduced under hydrogen flow at 673 K for 2 h (H$_2$ flow = 40 ml/min, heating rate = 8 K/min). The commercial catalyst 5 wt.% Rh supported on Al$_2$O$_3$ (Rh–Al$_2$O$_3$) (Engelhard) was supplied in reduced form and used without any further treatment.

X-ray diffraction analyses were carried out using a Philips PW 1319 diffractometer with Cu Kα

radiation. Adsorption–desorption experiments using N_2 were carried out at 77 K using a Micromeritics ASAP 2010. Before each measurement the samples were outgassed at 423 K and 1.33×10^{-3} Pa for 12 h. The N_2 isotherms were used to determine the surface area. The *t*-plot and DFT (density functional theory) methods were used to evaluate the micropore volume (V_μ) and the pore distribution, respectively. Hydrogen chemisorption measurements were performed using a Micromeritics Autochem 2910.

High resolution TEM micrographs were taken with a JEM 3010 (JEOL), operating at 300 kV. Few milligrams of the powder were gently ground in an agate mortar under high-purity *i*-propyl alcohol: the suspension was sonicated for 5 min, in order to further disrupt possible agglomerates. A 5 μl droplet of suspension was transferred onto a wholly amorphous carbon film, coating a 200 mesh copper grid (TAAB Laboratories Equipment), and let dry in a desiccator.

Catalytic tests were carried out using a 300 ml stainless steel Parr reactor equipped with a magnetic stirrer and digital oven temperature control instrument. The standard conditions for the experiments carried out were: 2.0 MPa H_2 pressure, 15.0 ml of quinoline, 135.0 ml of *i*-propanol and 0.450 g of Rh–Al_2O_3 or 1.125 g Rh–PLC catalyst (to maintain constant the quinoline/Rh weight ratio). The quinoline (98%) and *i*-propanol (98%) (Aldrich Chemicals) were used as received without any previous purification. Before heating, the autoclave was purged with helium at 0.3 MPa three times. When the system reached the reaction temperature, the hydrogen was introduced at the set pressure and the reaction started. The reaction mixtures were sampled after 150 min of reaction time and analyzed by gas chromatography using a Perkin Elmer Autosystem XL equipped with an PE-5 column (30 m × 0.25 mm, film thickness 0.25 μm) and FID detector. The yield reported are referred to the starting

quinoline and the qualitative analyses were carried out using a GC–MS Hewlett-Packard GCD 1800A system equipped with an HP-5 column (30 m × 0.25 mm, film thickness 0.25 μm) and mass spectrometer detector.

3. Results and discussion

Al/Ce/Mg pillared clays have a very high thermal stability [16]. It is well known that the thermal stability of pillared clays is related more to the composition of the pillars than to the type of clay used. With pure aluminum pillars, the structure collapses at $T = 723$ K, while Ce/Mg/Al pillared clays are stable up to 873 K. The main characterization data (d_{001} basal spacing, surface area, micropore volume and pore distribution) of the starting PLC support and Rh–PLC catalyst are reported in Table 1. The Rh–PLC catalyst shows the same basal spacing as that of the PLC and only a slight decrease in surface area and porosity. The wide angle XRD profiles of the Rh–PLC and the Rh–Al_2O_3 catalysts are reported in Figs. 2 and 3. The XRD profile of the inorganic supporting material, mainly in the case of alumina, is superimposed on the signals attributable to metallic Rh, nevertheless the sharp peaks of particles larger than 5 nm would have been detectable and, thus, their presence can be excluded in both samples before and after the reaction. The diameters of the metal particles before reaction, estimated by H_2 chemisorption, were 2 and 4 nm for Rh–PLC and Rh–Al_2O_3 catalysts, respectively (Table 2). The former finding has been confirmed also by high resolution TEM microscopy that showed the presence of Rh particles <2 nm on the surface of the Rh–PLC catalyst as prepared (Fig. 4). The hydrogenation of quinoline carried out at 373 K showed very different activities for the Rh–Al_2O_3 and Rh–PLC catalysts (Table 3, tests 1 and 2). After 150 min, the hydrogenation

Table 1
Basal spacing (d_{001}), surface area, pore volume, micropore volume (V_μ) and DFT pore volume distribution

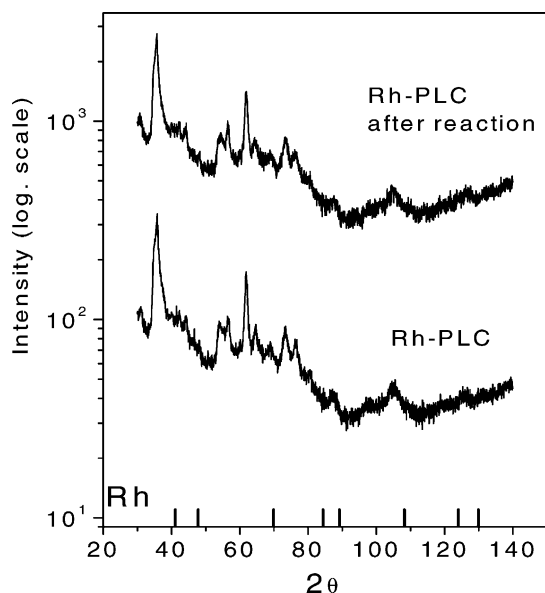|	d_{001} (nm)	Surface area (m^2/g)	Total pore volume (cm^3/g)	V_μ (cm^3/g)	DFT pore volume distribution (cm^3/g)		
					0–2 nm	2–10 nm	10–100 nm
PLC	1.8	269	0.192	0.063	0.070	0.060	0.062
Rh–PLC	1.8	194	0.190	0.053	0.051	0.043	0.096

Fig. 2. X-ray powder diffraction patterns of the Rh–PLC catalyst before and after the catalytic tests.
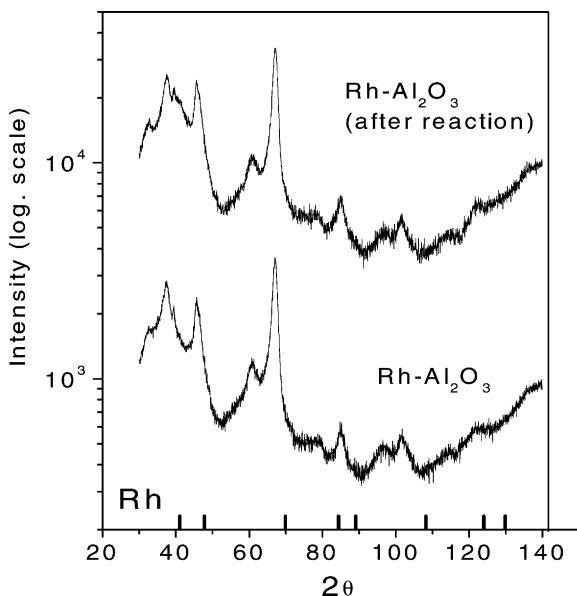

Fig. 3. X-ray powder diffraction patterns of the Rh–Al$_2$O$_3$ catalyst before and after the catalytic tests.

Table 2
Rh crystallite size determined by H$_2$ chemisorption for the catalysts before and after the catalytic tests

Catalyst	Rh crystallite size (nm)	
	Before	After
Rh–Al$_2$O$_3$	4	36
Rh–PLC	2	18

of quinoline using Rh–Al$_2$O$_3$ catalyst was almost complete and significantly higher than that obtained with the Rh–PLC catalyst. However, with both catalysts the main product was py-THQ, with very low amounts (yield $\leq$ 1%) of 5,6,7,8-tetrahydroquinoline (bz-THQ) as a by-product. In these conditions, the fully hydrogenated DHQ was not observed, probably as a result of catalyst deactivation due to adsorption of the intermediate(s) on the surface [11]. The lower activity obtained using the Rh–PLC catalyst may be attributed to the microporous nature of the pillared clay support and to the steric hindrance of the quinoline molecule that can consequently interact only with a small fraction of Rh, i.e. the metal crystallites present on the surface of the catalyst particles.

At temperatures higher than 373 K, the two catalysts showed completely different behaviors (Table 3).
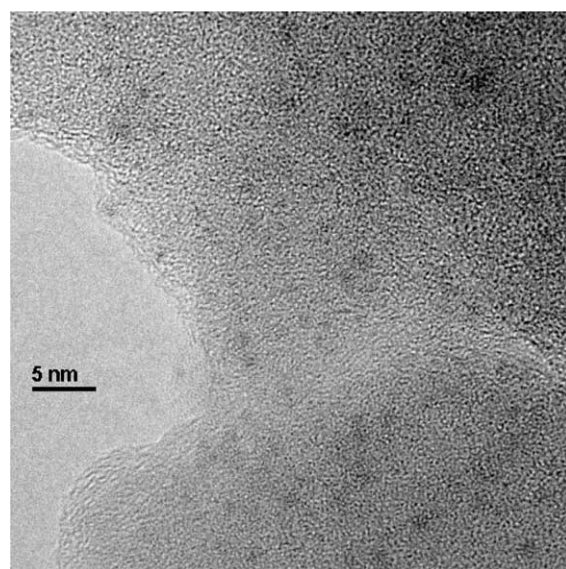

Fig. 4. High resolution micrograph of Rh–PLC catalyst before the catalytic tests (magnification 400,000×).

Table 3
Conversion of quinoline and yield in py-THQ and DHQ obtained using 5 wt.% Rh on Al_2O_3 (Rh–Al_2O_3) and 2 wt.% Rh on pillared layered montmorillonite (Rh–PLC) catalysts ($W_{Rh–Al_2O_3} = 0.450$ g; $W_{Rh–PLC} = 1.125$ g; quinoline $= 15.0$ ml; i-propanol $= 135.0$ ml; $P_{H_2} = 2.0$ MPa)

Test	Catalyst	Temperature (K)	Quinoline conversion (%)	Yield in py-THQ (%)	Yield in DHQ (%)
1	Rh–Al_2O_3	373	95.8	95.2	0.0
2	Rh–PLC	373	10.1	9.4	0.0
3	Rh–Al_2O_3	473	100.0	99.5	0.0
4[a]	Rh–PLC	473	99.9	49.6	41.9

[a] Yield in the by-products (%): *N*-2-propyl-quinoline (5.1), *N*-2-propyl-2-propyl-cyclohexylamine (2.3) and propyl-cyclohexane (traces).

At 473 K, the commercial catalyst showed only a slight increase in the quinoline conversion in comparison to the test carried out at the lower temperature, without any change in the selectivity (tests 1 and 3). On the contrary, the Rh–PLC catalyst exhibited not only the complete conversion of quinoline, but, surprisingly, also gave rise to a significant amount of the fully hydrogenated product (DHQ). This latter result is even more intriguing considering that at 473 K, Rh–PLC catalysts also formed a non-negligible amount of by-products (ca. 10%), attributable to the alkylation of DHQ by i-propanol (*N*-2-propyl-quinoline) followed by hydrogenolysis (*N*-2-propyl-2-propyl-cyclohexylamine and traces of propyl-cyclohexane). The increase of activity observed for the Rh–PLC catalyst in the range 373–473 K corresponded to an apparent activation energy ($E_{a_{app}}$) of about 110 kJ/mol, value sensibly higher to that attributable to a decrease of diffusion phenomena. Although, we were not able to keep in the literature a value of the $E_{a_{app}}$ for the complete hydrogenation of quindine to DHQ, it may be extrapolated on the basis of the data reported for benzene, naphthalene and pyridine [17–19]. Considering that moving from the hydrogenation of benzene to that of naphthalene a difference of $E_{a_{app}}$ of about 40 kJ/mol has been reported in the literature [17,18], a difference of ca. 50 kJ/mol between the $E_{a_{app}}$ for the hydrogenation of quindine and that of pyridine [19] may be considered reasonable.

XRD profiles of both the catalyst samples before and after the catalytic tests (Figs. 2 and 3) did not show significant increases in the size of the metal particles due to sintering phenomena, therefore the apparent decrease in the metal dispersion evidenced by H_2 chemisorption measurements for the samples after the catalytic tests (Table 2) has to be essentially attributed

to a reduction of the active surface caused by the adsorption of coke or other heavy products. However, it must be pointed out that after reaction, the size of the Rh crystallites in the Rh–PLC catalyst is smaller than in the commercial catalyst. This assumption was confirmed by high resolution TEM microscopy, which evidenced that in the Rh–PLC catalyst after the catalytic test all the particles visible on the catalyst surface had diameters ≤ 2 nm (Fig. 5). Therefore, the Rh particle size of the two catalysts before and after reaction (Table 2) indicates that the key parameter to obtain mild hydrogenation of quinoline to DHQ is the size of the Rh crystallites. An average particle size of about 2 nm may avoid any strong adsorption of reaction
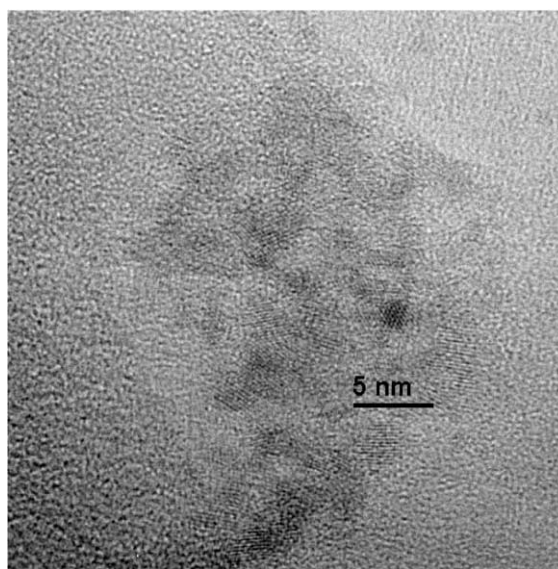

Fig. 5. High resolution micrograph of Rh–PLC catalyst after the catalytic tests (magnification 500,000×).

intermediate(s) and favor the further hydrogenation of py-THQ.

4. Conclusions

Highly dispersed noble metal containing catalysts may be obtained by ion-exchange of PLCs. Even though in these catalysts only the surface metal clusters are available for interaction with bulky substrates, they exhibit an interesting and unusual catalytic behavior. In particular, in the mild hydrogenation of quinoline, unlike that observed with a commercial Rh–alumina catalyst, using a Rh-exchanged PLC catalyst (Rh particle size $\leq$ 2 nm), it was possible to obtain a good yield in the fully hydrogenated product (DHQ). This latter result may shed light on the role of the metal particle size in the enantioselective hydrogenation using Pt–cinchonidine heterogeneous catalysts [12–15]. Thus, it may be hypothesized that the observed decrease in enantioselectivity with decreasing size of the metal particles is attributable to an increase in the hydrogenation of the quinolinic ring of the cinchonidine, rather than merely to a decrease in its adsorption on the catalyst surface [14].

Acknowledgements

References

[1] G. Perot, Catal. Today 10 (1991) 447.
[2] R.T. Shuman, P.L. Ornstein, J.W. Paschal, P.D. Gesellchem, J. Org. Chem. 55 (1990) 738.
[3] J.M. Schaus, D.L. Huser, R.D. Titus, Synth. Commun. 20 (1990) 3553.
[4] P. Bouyssou, C. Le Goff, J. Chenault, J. Heterocycl. Chem. 29 (1992) 895.
[5] C.W. Curtis, D.R. Cahela, Energy Fuels 3 (1989) 168.
[6] H. Adkins, H.R. Billica, J. Am. Chem. Soc. 70 (1948) 695.
[7] J.E. Shaw, P.R. Stapp, J. Heterocycl. Chem. 24 (1987) 1477.
[8] F. Santangelo, C. Casagrande, G. Miragoli, V. Vecchietti, Eur. J. Med. Chem. 20 (1994) 877.
[9] M. Freifelder, Adv. Catal. 14 (1963) 203.
[10] S. Tsushima, J. Sudzuki, J. Chem. Soc. Jpn. 64 (1943) 1295; Chem. Abstr. 41 (1947) 3801.
[11] M. Campanati, A. Vaccari, O. Piccolo, J. Mol. Catal. A, in press.
[12] Y. Orito, S. Imai, S. Niwa, Nippon Kagaku Kaishi 8 (1979) 1118; Chem. Abstr. 91 (1979) 192483h.
[13] G. Webb, P.B. Wells, Catal. Today 12 (1992) 319.
[14] J.T. Wehrli, A. Baiker, D.M. Monti, U. Blaser, J. Mol. Catal. 61 (1990) 207.
[15] S.D. Jackson, M.B.T. Keegan, G.D. McLellan, P.A. Meheux, R.B. Moyes, G. Webb, P.B. Wells, R. Whyman, J. Willis, in: G. Poncelet, P.A. Jacobs, P. Grange, B. Delmon (Eds.), Preparation of catalysts V, Studies in Surface Science and Catalysis, Vol. 63, Elsevier, Amsterdam, 1991, p. 135.
[16] C. Flego, L. Galasso, R. Millini, I. Kiricsi, Appl. Catal. A 168 (1998) 323.
[17] S.D. Lin, M. Albert Vannice, J. Catal. 143 (1993) 539.
[18] C.-M. Lu, Y.-M. Lin, I. Wang, Appl. Catal. A 198 (2000) 223.
[19] J.A. Anabtawi, R.S. Mann, K.C. Khulbe, J. Catal. 63 (1980) 456.